HiSST: 3rd International Conference on
High-Speed Vehicle Science Technology
14 -19 April 2024, Busan, Korea

Measurement method of thermal environment of reentry capsule

JIA Guangsen[1], YAO Dapeng[1], JIN Xin[1], LIN Jian[1], CHEN Nong[1]

Abstract

Accurate prediction of the thermal environment is crucial for the thermal protection design and safe return of the reentry capsule. In order to realize the measurement of temperature-sensitive paint at the bottom of the reentry capsule, the design method of the optical path in the direction of the flow and the correction algorithm of the non-uniform light intensity field were studied. The experimental results show that the embedded positive pressure instrument protection device not only effectively realizes the heat dissipation of the image acquisition equipment and the effective isolation from the vacuum environment, but also realizes the acquisition of temperature-sensitive paint images in the direction of the air flow. The correction algorithm improves the measurement accuracy of temperature-sensitive paint under the condition of large angle, and provides an effective experimental method for the measurement of temperature-sensitive paint in the thermal environment of the blunt head.

Keywords: *Reentry capsule; Temperature sensitive paint; Experimental method*

Nomenclature

I – light intensity
α – angle
ρ – density
c – specific heat capacity
k – Thermal conductivity
Ma – Mach number
P – pressure
Re – Reynolds number
V – Velocity
Subscripts
0 – stagnation condition
∞ – freestream conditions

1. introduction

For missions such as deep space exploration return and manned moon landing, reentry is the final stage of the entire mission. It is the ultimate symbol of the mission's success or failure, and also the most severe, complex, and dangerous part of the flight environment [1]. During the reentry process, the aircraft experiences severe aerodynamic heating due to its interaction with the surrounding air. This results in a sharp increase in the surface temperature of the aircraft, and even ablation, which is a crucial stage in the thermal load design of the reentry capsule. It is essential to accurately predict the aerodynamic thermal environment of each part of the aircraft and implement effective thermal protection measures. This is a critical technology for the design of high-speed aircraft.

To address the issue of measuring the thermal environment of high-speed aircraft, traditional experimental methods use point or integral heat flux sensors [2]. However, these methods only provide heat flux distribution at discrete points, and can potentially damage the surface structure of the model and interfere with the flow field. Thermography technology utilises a non-contact measurement method to obtain large area heat flux data without disturbing the flow field. It has become an important direction for the development of heat flux measurement technology [3].

[1] *China Academy of Aerospace Aerodynamic, 17#, Yungang West Road, Beijing, 100074, China, jgs1014@163.com*

Currently, temperature-sensitive paint has become the standard technology for aerothermal experiments at NASA Langley Centre. NASA has established a temperature-sensitive paint measurement system in several hypersonic wind tunnels, including the 20-inch M6 wind tunnel, 31-inch M10 wind tunnel, and 20-inch CF4 wind tunnel. This system is widely used in the aerothermal environment research of X33, X34, X38, CEV, and other project models [4-6]. Additionally, the French Aerospace Research Institute has conducted research on technology that uses two-color temperature-sensitive paint [7].

The technology of temperature-sensitive paint typically utilises the observation window located on the side of the wind tunnel test section to capture data. This method only allows for the collection of heat flux distribution on the side of the aircraft [8-9]. The thermal environment in the area of the large, blunt head and return capsule is poor, primarily due to the difficulty of capturing images and measuring temperatures in this region. Additionally, the large curvature surface significantly impacts the radiation intensity of the temperature-sensitive material. This paper presents a method for measuring the temperature-sensitive paint of the head of the large blunt head of the reentry capsule. To achieve this, a positive pressure instrument chamber is designed, and the correction method of the radiant intensity at the large polar angle is studied. Additionally, the heat flux distribution at the bottom of the return capsule is measured.

2. Measurement method

2.1. Measuring principle of temperature-sensitive paints

Temperature-sensitive paints utilise the photoluminescence and thermal quenching effects of temperature-sensitive materials to measure surface heat flux [10-12]. The material is excited and emits visible light when irradiated with a specific wavelength of light. The radiant light intensity weakens with increasing temperature due to the thermal quenching effect of the material. The temperature of an object's surface can be determined by measuring the change in radiant light intensity. Integrating the temperature over time allows for the acquisition of heat flux information for the model surface, as shown in Figure 1.

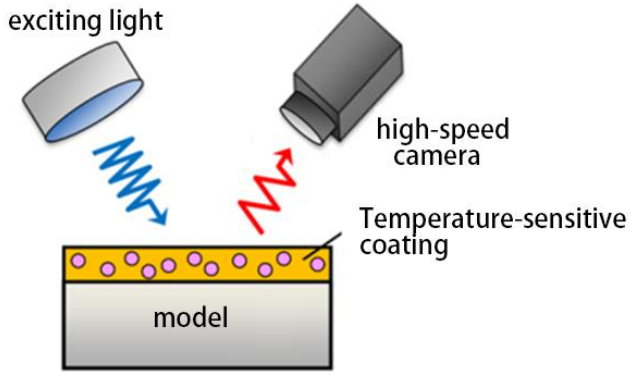

Fig 1. Measuring principle of temperature-sensitive paints

2.2. Image acquisition methods

In order to measure the heat flux at the bottom of the capsule using temperature-sensitive paint, the camera must capture an image of the capsule's underside. Additionally, the test section is subject to impact forces during wind tunnel operation, resulting in significant axial displacement. Therefore, the camera acquisition system must be effectively isolated from the test section. Three optical path schemes have been designed for this purpose, as illustrated in Figure 2(a). The first option involves installing a mirror in the wind tunnel test section to reflect the image from the bottom of the re-entry capsule onto the camera lens. In the second scheme, depicted in Figure 2(b), the camera, excitation light source, and other equipment are installed in a sealed chamber within the test section. In the third scheme, illustrated in Figure 2(c), the camera, excitation light source, and other equipment are installed within the test section embedded in the cabin and connected to the external atmosphere through the front wall of the test section.

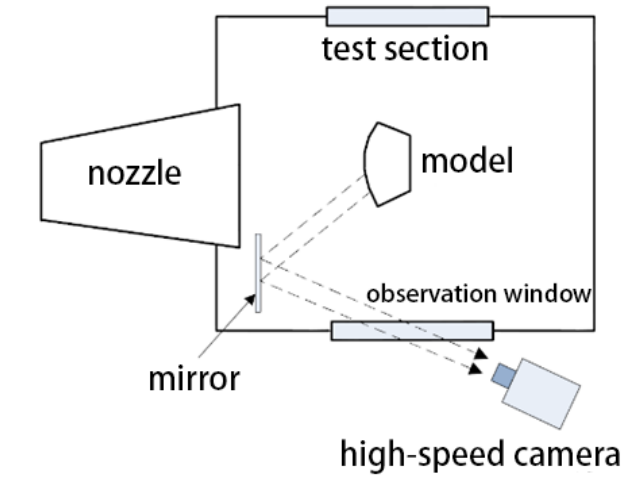

(a) Reflector scheme

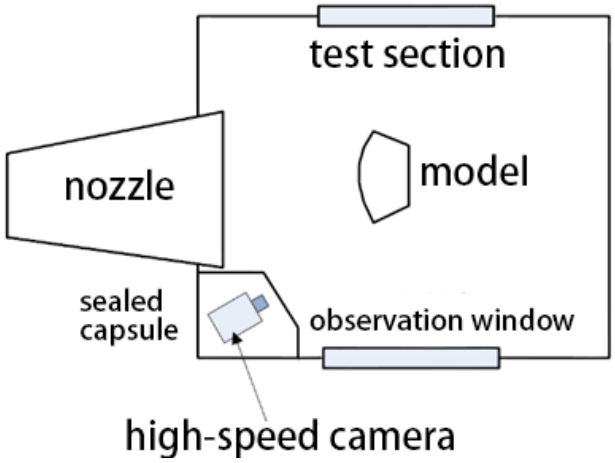

（b）Interior sealed chamber scheme

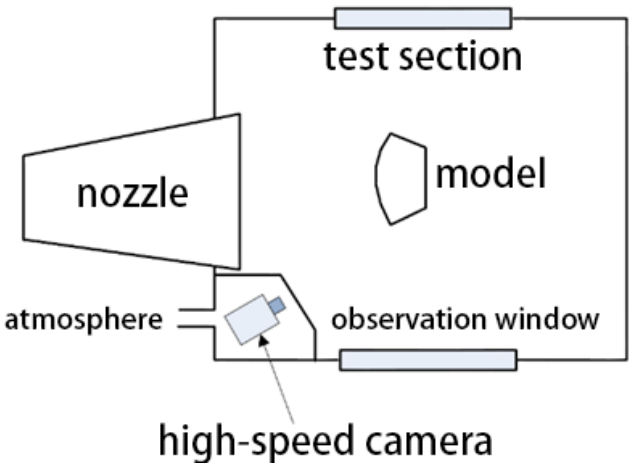

（c）Connecting cabin scheme

Fig 2. Different methods of image acquisition

The mirror is bolted to the inner wall of the test section, and the sharp cones is used for testing, as shown in Figure 3. The images of the whole experimental process were continuously taken, and it was found that the test section was affected by the impact during the experiment, resulting in a large axial translation, and the position of the mirror moved with the test section, which caused a large displacement of the model image, and the whole shooting field of view and model attitude changed

significantly, which could not meet the experimental needs. The camera and the excitation light source are placed in the sealed chamber in the test section, which can effectively isolate the camera from the vacuum in the test section, and play a good role in protecting the camera. Everything was fine at the beginning of the experiment, however, as the time of the experiment increased, the image showed so much noise that it was not even possible to resolve the image, as shown in Figure 4. After opening the sealed cabin, it was found that the high-speed camera could not dissipate heat in a closed environment, and the temperature in the cabin increased sharply with time, which significantly increased the thermal noise of the camera chip. Therefore, on the basis of the second scheme, the camera sealed cabin is connected with the outside atmosphere through the front end of the test section, and a heat dissipation fan is added at the outlet, so that the air in the sealed cabin circulates with the outside world, and the temperature in the cabin is reduced. At the same time, in order to prevent the vibration of the test section from affecting the camera, a separate row frame structure was established outside the test section, and the camera platform in the cabin was passed through the horizontal support rod.

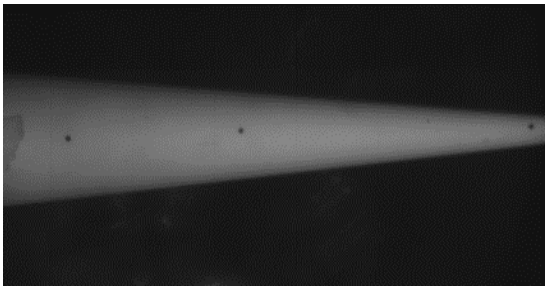

(a)wind off

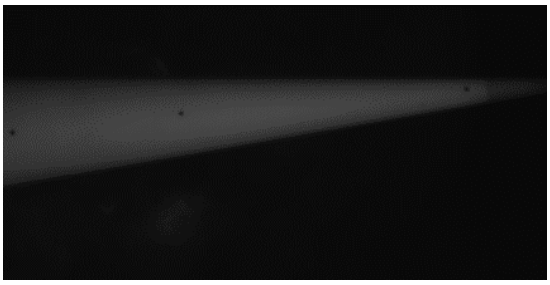

(b)wind on

Fig 3. Reflector scheme test image

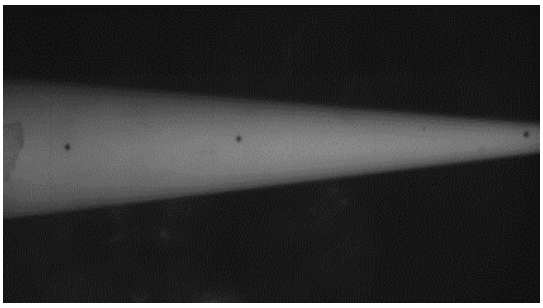

(a) Acquisition image at the beginning

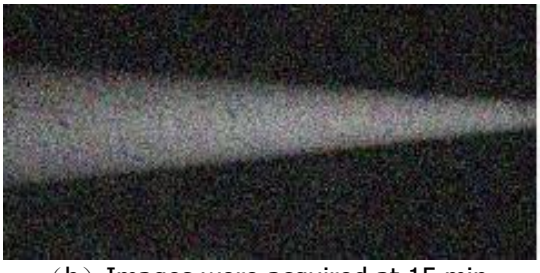

（b）Images were acquired at 15 min

Fig 4. Test image of the interior sealed chamber scheme

2.3. Shooting angle correction

Although the optical path system was redesigned, the camera axis still had a 45° angle with the bottom of the capsule. Therefore, we studied the influence of the camera shooting angle on the radiation intensity. Figure 5 shows a semicircular ceramic calibration device designed for this purpose. The device is composed of a flexible heating band, a ceramic arc, and a back tightening device. During calibration, the temperature-sensitive coating is sprayed onto the curved ceramic surface. The flexible heating belt is then fixed with a back tensioning device, and the change and distribution of radiation intensity are measured by the camera while heating. The test results show that the shooting angle within 40° has a relatively small effect on the light intensity. However, after 40°, the light intensity drops significantly.

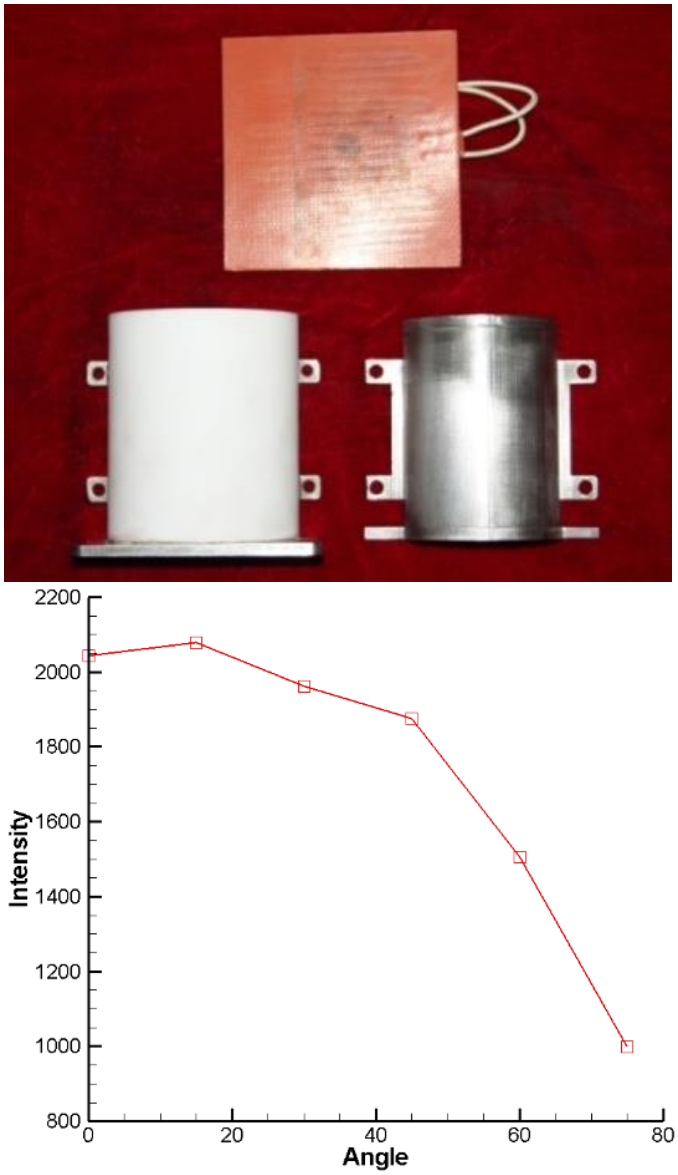

Fig.5 The calibration device with the change of light intensity with curvature and the relationship curve between shooting angle and light intensity

In order to eliminate the influence of the shooting angle, it is assumed that the change of light intensity has the following functional relationship with the included angle:

$$\frac{I}{I_{\max}} = f(\alpha) \qquad (1)$$

$I_{\max}$ is the light intensity of the vertical camera axis, I is the surface light intensity of the curved surface calibration device, α is the angle between the surface normal of the surface calibration device and the camera axis.

Considering the actual needs of the project, the quadratic polynomial is used to fit the function, and the following results are:

$$f(\alpha) = -0.0001\alpha^2 + 0.0041\alpha + 0.986 \quad (2)$$

It can be seen from Ref. 13 that the rate of change of radiant light intensity of temperature-sensitive materials is linearly related to temperature.

$$T(\tau) = k(\frac{I}{I_0}) + 1 \quad (3)$$

After considering the influence of the included angle, the equation above can be modified as follows:

$$T(\tau) = k(\frac{I}{I_0 * f(a)}) + 1 \quad (4)$$

2.4. Method for calculating heat flux

Under the assumption of one-dimensionality and semi-infiniteness, the relationship between surface temperature change and wall heat flux during transient heat transfer is expressed as follows [13-15]:

$$q_w(t) = \sqrt{\frac{k\rho c}{\pi}}\left[\frac{T(t)}{\sqrt{t}} + \frac{1}{2}\int_0^t \frac{T(t)-T(\tau)}{(t-\tau)}d\tau\right] \quad (5)$$

Where $q_w(t)$ is the surface heat flux and ρ, c, and k are the density, specific heat capacity, and thermal conductivity of the model material, respectively.

3. Experimental setup

3.1. Flow parameters

The experiment took place in the shock wave wind tunnel at the China Academy of Aerospace Aerodynamics. The experimental parameters are presented in Table 1.

Table 1. Flow parameters

Ma	P_0(MPa)	T_0(K)	*Re*（/m）	v_∞m/s）	ρ_∞(kg/m^3)
6.08	1.5	690	1.0E+07	1268	0.0356

3.2. model

The Crew Exploration Vehicle is the experimental model, as shown in Figure 6. In addition to using temperature-sensitive paint, several thermocouples are arranged at the 0° and 180° meridians at the bottom of the capsule.

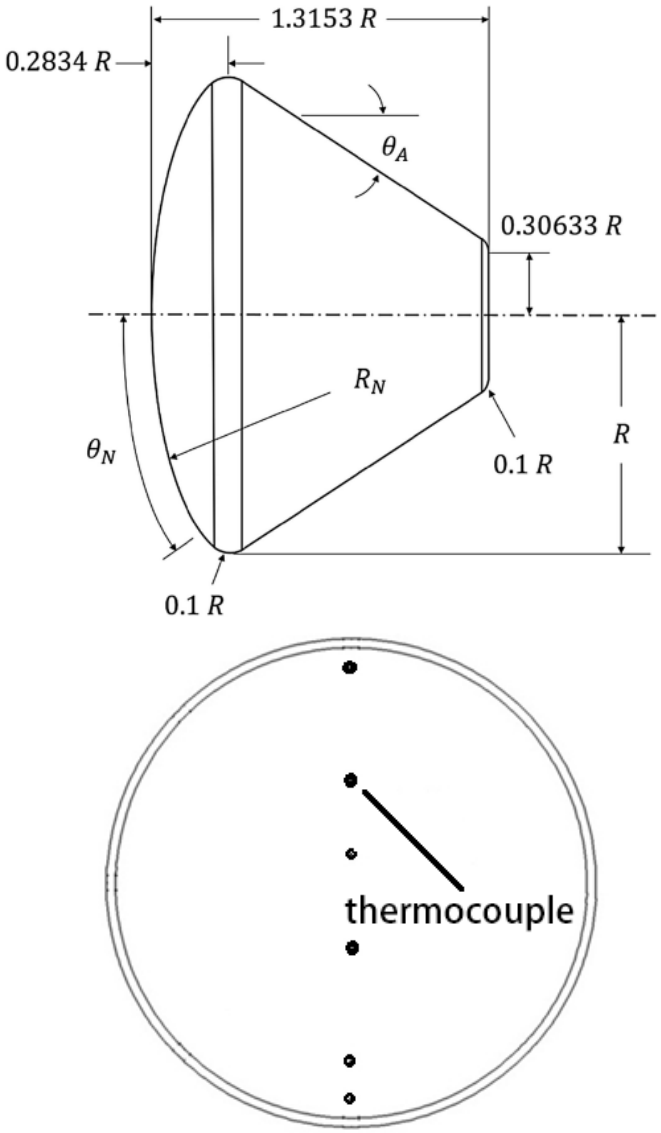

Fig.6 Experimental model and sensor arrangement

where，R=150mm， $R_N = 2.4R$ ， $\theta_A = 32.5°$ ， $\theta_N = 23.04°$ 。

4. Results and discussion

Figure 7 shows the distribution of heat flux at the bottom of the re-entry capsule at different angles of attack. Additionally, Figure 8 compares the measurement data of the temperature-sensitive paint with the sensor data. At Mach 6, the bottom surface of the re-entry capsule is fully turbulent, and the heat flux in the area near the station reaches about twice the calorific value of the ball head of the same diameter. The highest heat flux in the shoulder region typically occurs in front of the physical shoulder. Following a change in the angle of attack, the area of high heat flux on the underside is noticeably shifted towards the side facing the wind, resulting in a decrease in heat flux on the opposite side and a significant increase in heat flux on the wind-facing shoulder.

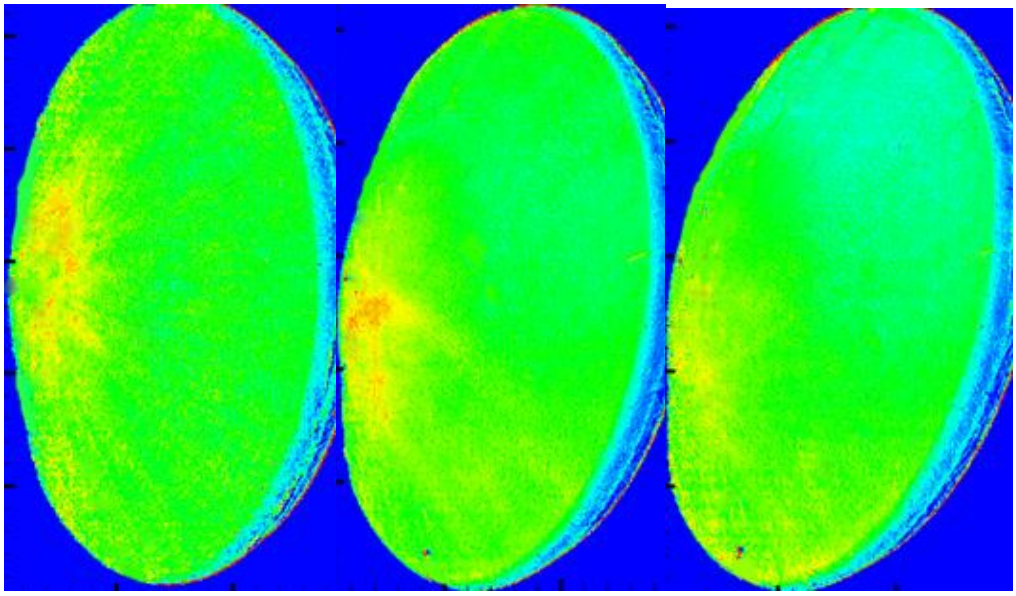

(a) Angle of attack=0° (b) Angle of attack=8° (a) Angle of attack=16°

Fig.7 Results of temperature-sensitive paint at different angles of attack

The temperature-sensitive paint measurement results are compared with the sensor results, as illustrated in Figure 8. Overall, the temperature-sensitive paint measurement results are consistent with the sensor results in terms of the heat flux distribution law at the bottom and the heat flux value. At an angle of attack of 0°, the heat flux is highest in the middle and gradually decreases towards both sides. The local peak heat flux occurs when it reaches the shoulder. As the angle of attack increases, the area of high heat flux shifts to one side. The temperature-sensitive paint measurement technology effectively captures the variation of heat flux at the bottom of the return capsule with the angle of attack. The difference with the sensor is within 10%.

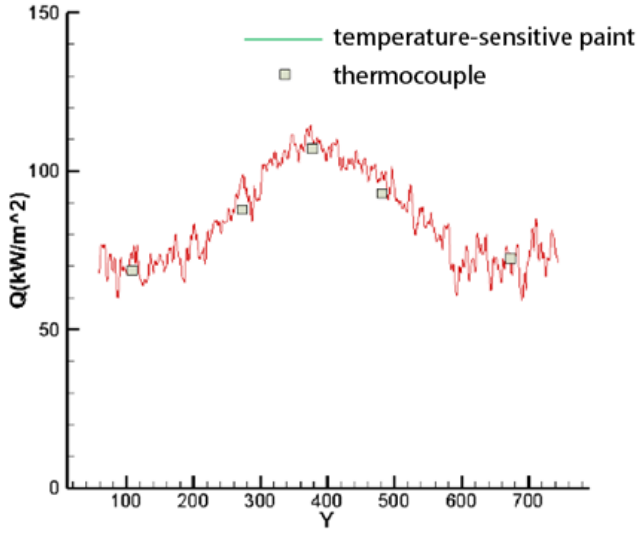

(a) Angle of attack=0°

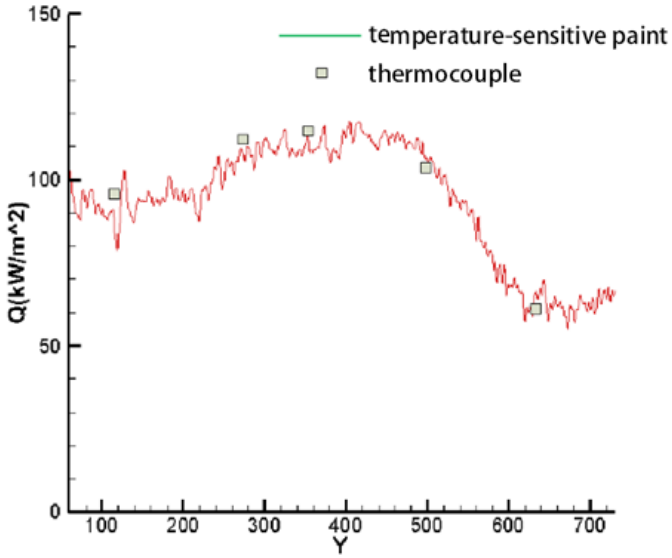

(b) Angle of attack=8°

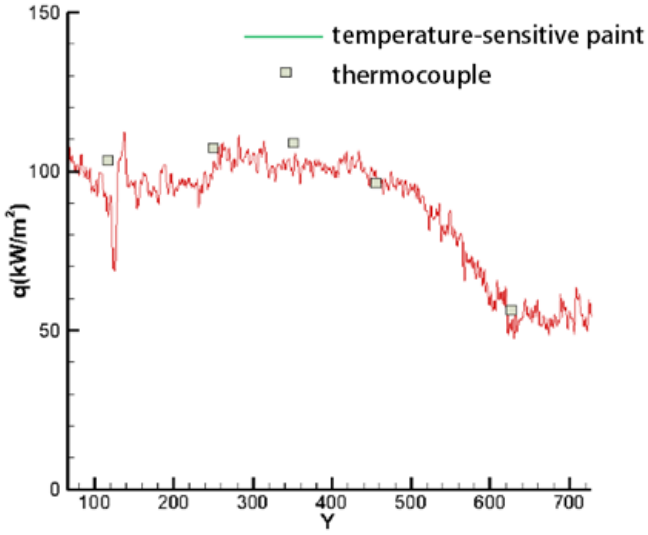

(c) Angle of attack=16°

Fig.8 Comparison of temperature-sensitive paint and thermocouple

5. Conclusion

This paper presents a camera installation and shooting scheme to measure the thermal environment at the bottom of the re-entry capsule and the large blunt head body using temperature-sensitive paint technology. The study investigates the variation law of the radiant light intensity of the temperature-sensitive material at the large polar angle and provides the corresponding correction algorithm. Wind tunnel experiments are conducted using the shape of the Orion re-entry capsule. The language used is clear, concise, and objective, with a formal register and precise word choice. The text adheres to conventional structure and format, with consistent citation and footnote style. The grammar, spelling, and punctuation are correct. No changes in content have been made. The experimental results indicate that the positive pressure protection device embedded in the image acquisition equipment can effectively dissipate heat and isolate it from the near-vacuum environment. This enables the acquisition of experimental images in the direction of the air flow. The optimization algorithm enhances the precision of surface measurement even at large angles, providing an effective experimental method for measuring the thermal environment at the bottom of the reentry capsule.

References

1. Zhang Zhicheng, Pan Meilin, Liu Chuping." Hypersonic aerothermal and thermal protection." (2003).
2. LIU Chuping, ed. Heat flux measurement in aerothermal and thermal protection tests. National Defense Industry Press, (2013).
3. Bradley, Lee C. A Temperature‐Sensitive Phosphor Used to Measure Surface Temperatures in Aerodynamics. *Review of Scientific Instruments* 24.3 (1953): 219-220.
4. Czysz, Paul, and W. Paul Dixon. Quantitative heat transfer measurement using thermographic phosphors. *Optical Engineering* 7.3 (1969): 77-79.
5. Buck, G. Surface temperature/heat transfer measurement using a quantitative phosphor thermography system. *29th Aerospace Sciences Meeting*. 1991.
6. Merski, N. Ronald. Global aero heating wind-tunnel measurements using improved two-color phosphor thermography method. *Journal of Spacecraft and Rockets* 36.2 (1999): 160-170.
7. Jones, Michelle L., and Scott A. Berry. Thermographic Phosphor Measurements of Shock-Shock Interactions on a Swept Cylinder. *Thermal and Fluids Analysis Workshop (TFAWS 2013)*. No. NF1676L-16678. 2013.
8. Miller, C. Langley hypersonic aerodynamic/aerothermodynamic testing capabilities-present and future.*16th Aerodynamic Ground Testing Conference*. 1990.
9. Berry, Scott, Robert Nowak, and Thomas Horvath. Boundary layer control for hypersonic airbreathing vehicles.*34th AIAA Fluid Dynamics Conference and Exhibit*. 2008.
10. Le Sant, Y., and J. L. Edy. Phosphor thermography technique in hypersonic wind tunnels: First results. *International Congress on Instrumentation in Aerospace Simulation Facilities.* IEEE, 1993.
11. Hubner, J. P., et al. Temperature-and pressure-sensitive paint measurements in short-duration hypersonic flow. *AIAA journal* 39.4 (2001): 654-659.
12. Nakakita, Kazuyuki, Tatsuya Osafune, and Keisuke Asai. Global heat transfer measurement in a hypersonic shock tunnel using temperature-sensitive paint.*41st Aerospace Sciences Meeting and Exhibit*. 2003.
13. Bi Zhixian, et al. Research on Phosphor Thermography. Journal of Experimental Fluid Mechanics 27.3 (2013): 87-92.
14. Zhixian Bi, et al. Application of Phosphor Thermography in surface heat flux measurement experiment of X-33 aircraft. Xi'an: Chinese Mechanics Congress (2013).
15. Jiasui Zhou, et al. Preliminary Experimental Study on Temperature-Sensitive paint in Shock Wave Wind Tunnel. Journal of Experiment Fluid Mechanics 27.5 (2013): 79-82.